Identification of a myeloid-derived suppressor cell cystatin-like protein that inhibits metastasis

Angela M. Boutté,* David B. Friedman,[†] Matthew Bogyo,[‡] Yongfen Min,[§] Li Yang,[§] and P. Charles Lin[§,1]

*Department of Cancer Biology and [†]Department of Biochemistry, Vanderbilt University Medical Center, Nashville, Tennessee, USA; [‡]Department of Pathology, Stanford University School of Medicine, Stanford, California, USA; and [§]Center for Cancer Research, National Cancer Institutes, Bethesda, Maryland, USA

ABSTRACT   Myeloid-derived suppressor cells (MDSCs) are significantly increased in cancer patients and tumor bearing-animals. MDSCs infiltrate into tumors and promote tumor invasion and metastasis. To identify the mediator responsible for the prometastatic property of MDSCs, we used proteomics. We found neutrophilic granule protein (NGP) was decreased >2-fold in MDSCs from metastatic 4T1 tumor-bearing mice compared to nonmetastatic 67NR controls. NGP mRNA levels were decreased in bone marrow and in tumor-infiltrating MDSCs by 45 and 66%, respectively, in 4T1 tumor-bearing mice compared to 67NR controls. Interestingly, 4T1-conditioned medium reduced myeloid cell NGP expression by ~40%, suggesting that a secreted factor mediates gene reduction. Sequence analysis shows a putative cystatin domain in NGP, and biochemical analysis confirms NGP a novel cathepsin inhibitor. It inhibited cathepsin B activity by nearly 40% *in vitro*. NGP expression in 4T1 tumor cells suppressed cell invasion, delayed primary tumor growth, and greatly reduced lung metastasis *in vivo*. A 2.8-fold reduction of cathepsin activity was found in tumors expressing NGP compared to controls. NGP significantly reduced tumor angiogenesis to 12.6 from 19.6 and lymphangiogenesis to 4.6 from 9.1 vessels/field. Necrosis was detectable only in NGP-expressing tumors, and the number of apoptotic cells increased to 22.4 from 8.3 in controls. Taken together, this study identifies a negative regulator of tumor metastasis in MDSCs, NGP, which is down-regulated in metastatic conditions. The finding suggests that malignant tumors promote invasion/metastasis not only through up-regulation of proteases but also down-regulation of protease inhibitors.—Boutté, A. M., Friedman, D. B., Bogyo, M., Min, Y., Yang, L., Lin, P. C. Identification of a myeloid-derived suppressor cell cystatin-like protein that inhibits metastasis. *FASEB J.* 25, 000–000 (2011). www.fasebj.org

Key Words: cathepsin · angiogenesis · lymphanogenesis · NGP

IN ADDITION TO TUMOR CELLS themselves, the tumor microenvironment contains a variety of host-derived cells, including infiltrating inflammatory cells. These cells facilitate tumor angiogenesis, progression, and metastasis. Myeloid-derived suppressor cells (MDSCs) are bone marrow-derived myeloid cells that express cell surface antigens Gr-1 and CD11b in mice. These cells are increased significantly in bone marrow and spleens of animals bearing large tumors; MDSCs suppress host immune function under tumor conditions (1). These cells are found in the peripheral blood of patients with cancer and are correlated positively to malignancy (2), which suggests that MDSCS have a role in tumor invasion and metastasis. MDSCs infiltrate into tumors and accumulate at the invasive front; they promote tumor angiogenesis through regulation of VEGF bioavailability as well as tumor cell invasion and metastasis *via* regulation of protease activities (3). MDSCs also confer resistance to cancer therapies (4). Hence, MDSCs are a viable target for therapeutic intervention.

Cathepsins are a family of cysteine proteases that regulate tumor development during angiogenesis, apoptosis, cell invasion, and metastasis. Cysteine cathepsin activity is elevated at the invasive fronts of carcinomas, has been implicated directly in metastasis, and is increased within the angiogenic vasculature, exacerbating angiogenesis and tumor growth (5). Cathepsins are also correlated positively to increased lymph node and distant metastasis in patients (6). Cystatins are endogenous cysteine cathepsin inhibitors (7). Epigenetic loss or modification of cystatins is correlated to unfavorable cancer prognosis (8) and to tumor growth and metastases (9). Conversely, cathepsin B ablation or overexpression of cystatins significantly slows tumor growth, reduces lung metastasis, and hinders tumor cell invasion and malignancy (10). Lastly, overexpression and increased activity of cathepsin B in the PymT mammary tumor model led to increased primary tumor weight,

increased angiogenesis, greater influx of immune derived cells, and more severe lung metastasis (11).

Neutrophilic granule protein (NGP) was identified initially in immature bone marrow cells and promyelocytes. This 19-kDa myeloid granule protein shares 30% similarity to cathelicidins, which are proteins within the cystatin superfamily (12). In addition, NGP gene expression has been reported to be controlled by C/EBP-ε and Pu.1 transcription factors, which might be similar to other myeloid genes (13). However, the molecular function of NGP *in vitro* and *in vivo* is currently unknown.

Although the importance of MDSCs in tumor progression and metastasis is quite evident, the molecular mechanism by which MDSCs achieve this feat is still unclear. Mass spectrometry based proteomics is an increasingly valuable tool in discovery of novel mediators, or biomarkers, of disease. Difference in gel electrophoresis (DIGE) provides a wide dynamic range of protein abundance detection and direct semiquantitative analysis.

This study utilized proteomic analysis of MDSCs associated with tumor metastasis to identify NGP. NGP was down-regulated in MDSCs isolated from metastatic compared to nonmetastatic hosts. Ectopic expression of NGP inhibited cathepsin B activity, hindered tumor cell invasion, and decreased lung metastasis. This study identified NGP, a potential type II cystatin and cathepsin B inhibitor, as an anti-invasion, antimetastasis, and antiangiogenic protein derived from MDSCs.

MATERIALS AND METHODS

Chemicals and cell lines

Murine NGP and cathepsin B cDNA was purchased from Open Biosystems/ThermoFisher (Huntsville, AL, USA); PCNA antibody from Santa Cruz Biotechnology (Santa Cruz, CA, USA); V5 antibody from Invitrogen (Carlsbad, CA, USA); Cyanine dyes and IPG strip pH gradient gels from GE Healthcare (Piscataway, NJ, USA); primers for β-actin, NGP, and V5-His$_6$ from Sigma-Genosys (St. Louis, MO, USA); Cathepsin B Innozyme fluorescent kit from EMD Chemicals (Gibbstown, NJ, USA).

HEK293T, NIH-3T3, 67NR, and 4T1 cells were maintained in DMEM supplemented with 10% FBS. Full-length NGP cDNA was subcloned into the pcDNA 3.1 vector fused with a C-terminal V5-His$_6$ tag. The DNA sequence was verified in house. The cells were transfected with either empty vector (Vec) pcDNA 3.1 or NGP-pcDNA 3.1 using Lipofectamine 2000 (Invitrogen) for 48 h. 4T1 stable cell lines were selected using G418 (Invitrogen). 32D cells were maintained in RPMI supplemented with 10% FBS and 4ng/ml recombinant mouse IL-3.

MDSC purification and mass spectrometry

For all purifications, single-cell suspensions were prepared from fresh bone marrow, spleen tissue, or tumor tissue harvested from mice with 4T1 and 67NR primary tumors similar to those described previously (3). Gr1$^+$/CD11b$^+$ cells were sequentially selected with magnetic anti-Gr1 and anti-

CD11b antibody beads (Miltenyi Biotec, Auburn, CA, USA). Purity of cell populations was confirmed by FACS using anti-Gr-1 FITC and anti-CD11b PE-conjugated antibodies.

For proteomics, spleen MDSC lysates were labeled with cyanine dye Cy3 and Cy5, employing dye switching. A standard mixture was labeled with Cy2. Equal ratios of samples were combined and separated simultaneously by isoelectric focusing in the first dimension, then PAGE in the second dimension, using 4 replicate gels. Coresolved protein spots were detected and quantitated with DeCyder (GE Healthcare), and statistical analysis was performed using Student's *t* test. The average standardized fold change is derived from 4 spots in 4 replicate gels, $n = 16$. One gel was poststained with SYPRO Ruby, and individual spots were isolated for MALDI-TOF/TOF or tandem mass spectrometry analysis as described previously (14).

Real-time RT-PCR and Western blotting

RNA was isolated from either 32D cells, 4T1 cells, or tumor tissue-derived MDSCs purified from bone marrow 67NR or 4T1 using the Qiagen RNEasy Kit (Qiagen, Valencia, CA, USA) and subjected to real-time PCR. C_T values were determined using SYBR Green and an iCycler or MyiQ instrument (Bio-Rad, Richmond, CA, USA). The NGP primer set for transcript detection was used as described previously (13). β-Actin was used as an internal control. For bone marrow and tumor MDSCs, we normalized the reading from the 67NR samples as 1 and then calculated the relative levels of NGP in 4T1 samples. Transcript abundance was determined using the $\Delta\Delta C_T$ method. All Western blots were performed according to manufacturers' instructions with NuPage reagents (Invitrogen). Film and fluorescence densitometry of scanned gels or Westerns was measured with Image J (U.S. National Institutes of Health, Bethesda, MD, USA).

Animal tumor models

All mice used in this work were housed in pathogen-free units at Vanderbilt University Medical Center, in compliance with Animal Care and Use Committee regulations. Female Balb/c mice (6–7 wk old) were purchased from Harlan Laboratories (Indianapolis, IN, USA). 4T1, 4T1-Vec, or 4T1-NGP cells (5×10^5 cells/mouse) were injected into the fourth mammary fat pad as described previously. Tumor growth was measured 2–3×/wk with a caliper over the time course indicated. In a separate cohort, primary tumors were allowed to grow for 2–3 wk. Mice with similarly sized primary tumors were selected for surgical removal. The mice were sacrificed 4 wk later, and fresh lungs were weighed, examined for metastases, and then fixed in Bouin's fixative prior to hematoxylin and eosin (H&E) staining. The number and size of metastatic tumors were measured manually by microscopic examination.

Cathepsin B enzymatic assay

For *in vitro* analysis, cells were lysed with cold Cytobuster Protein Extraction Reagent (EMD Chemicals). Inhibition of endogenous cathepsin B activity was determined after transfection of cells with an NGP vector using the Innozyme kit (EMD Chemicals). In a separate cohort, cells were transfected with cathepsin B, NGP, or empty vector controls. Cell lysates containing cathepsin B were mixed with lysates containing NGP or vector prior to measuring cathepsin B activity.

For *in vivo* imaging of cathepsin activity, 250 μM GB123 probe was injected intravenously 3 wk after tumor cell implantation, 1 d prior to sacrificing the animals as described previously. Live imaging was acquired using Xenogen IVIS

200 imaging system (Caliper Life Sciences, Hopkinton, MA, USA) equipped with a Cy 5.5 filter, followed by imaging of surgically excised tumors *ex vivo*. Tumor tissue lysates were separated by 4–12% SDS-PAGE, and images of GB123 bound cathepsin were acquired using the Odyssey Imaging System (Li-COR, Lincoln, NE, USA). Comparative band intensity was measured using Image J.

Protein alignment and dendrogram

Protein sequence alignment and dendrograms were generated using Clustal_X (http://www.clustal.org). NJPlot (http://pbil.univ-lyon1.fr/software/njplot.html) was used to display dendrogram results. By default, protein sequences are colored by residue as follows: orange, GPST; red, HKR; blue, FWY; green, ILMV.

Statistical analysis

Two-dimensional DIGE proteomic data was analyzed using the Student's *t* test with Benjamini-Hochberg correction by DeCyder (GE Healthcare). All other data were analyzed using Prism (GraphPad, La Jolla, CA, USA). All values are expressed as means ± SE. Real-time PCR, invasion, recombinant cathepsin B activity, GB123 probe binding intensity, cathepsin B immunoreactivity, and CD31, LYVE-1, or TUNEL immuno-fluorescence of tumor sections was analyzed paired by *t* test. Cathepsin B activity, NGP dose curve and tumor cell growth kinetics, and *in vivo* tumor growth were compared by ANOVA. For all tests, a value of $P < 0.05$ was considered significant.

RESULTS

Proteomic identification of a cystatin-like protein, NGP, in MDSCs negatively correlated to tumor metastasis

To identify the molecular mediators in MDSCs responsible for tumor metastasis, we used gel-based proteomics to profile proteins that were differentially expressed in MDSCs isolated from hosts bearing nonmetastatic or metastatic mammary tumors. 67NR and 4T1 cells are 2 cell lines originally derived from the same parental mammary adenocarcinoma. Although growth kinetics of the primary tumor are similar, these cells differ greatly in metastatic potential. 4T1 cells are highly metastatic, while 67NR cells only form primary tumors (15). MDSCs were isolated from spleens of mice bearing similarly sized tumors, pooled from 7 mice/group, and purified by magnetic cell sorting using antibodies against Gr-1 and CD11b. We achieved >94% purity as indicated by FACS analysis (Supplemental Fig. S1*A*).

MDSC protein lysates were differentially labeled with CyDyes and analyzed by DIGE. Using 4 replicate gels, protein spots from a standard mixture were used to normalize the intensity of comigrating regions of interest. This study sought to define the most obvious changes based on statistical criteria. Multiple spots identifying NGP were unambiguously identified by TOF/TOF and showed a significant ≥2-fold change ($P<0.01$) at ~20 kDa and pI ~ 6 (**Fig. 1***A*). The 3-dimensional view of protein spots 1–4 shows the intensity change between the nonmetastatic (67NR) and metastatic (4T1) tumor-bearing mice (Fig. 1*B*). The standardized average fold change, based on the differential signal intensity from 4 spots within 4 replicate gels, of NGP is −2.37 in MDSCs from 4T1 tumor-bearing mice compared to those bearing 67NR tumors (Fig. 1*C*). This result was significant by Student's *t* test ($P<0.0001$ or <0.002 with Benjamini-Hochberg false discovery rate). The amino acid sequence of peptide AIEAYNQGR was confirmed by peptide mass fingerprinting and tandem mass spectrometry (Supplemental Fig. S1*B*). We determined that the expression of NGP in MDSCs is negatively associated with tumor metastatic potential.
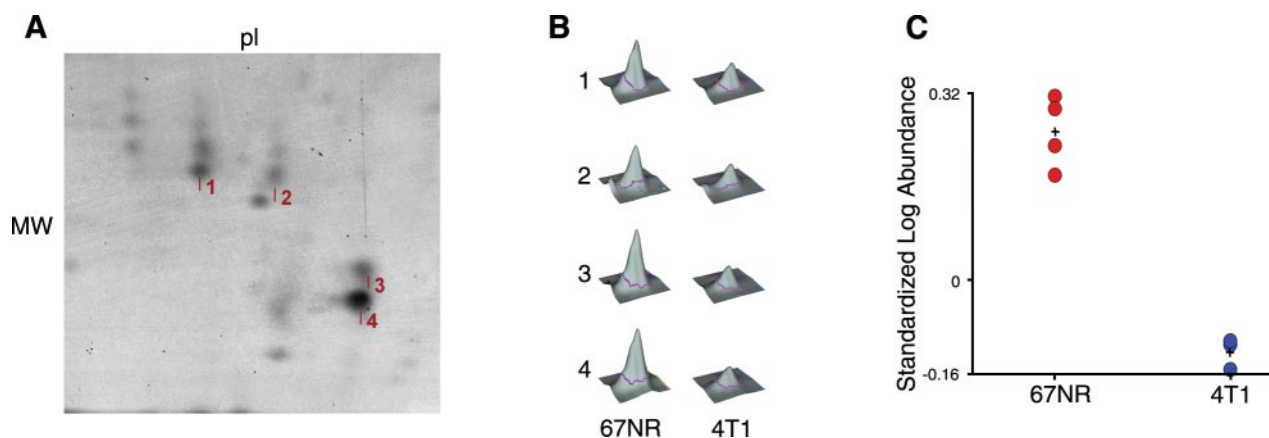

Figure 1. DIGE of NGP in MDSC lysates. Purified Gr1+/CD11b+ MDSCs isolated from spleen of mice bearing 4T1 tumors and 67NR tumors were analyzed by 2-dimensional gel electrophoresis. *A*) Representative image of a Sypro ruby-stained replicate gel for the migratory region of NGP. Protein spots 1–4 represent the NGP protein in the range of ~20 kDa and pI ~5. *B*) Peak intensity illustrations of peptide AIEAYNQGR from NGP isolated from 4 comigrating spots indicated in *A*. *C*) Graphical representation of the standardized log abundance of NGP protein spots 1–4 indicated in *A*. $P = 0.000028$ by Student's *t* test; $P = 0.0014$ with Benjamini-Hochberg false discovery rate correction. MDSC cell lysates were pooled from 6–7 mice/group and analyzed with 4 replicate gels.
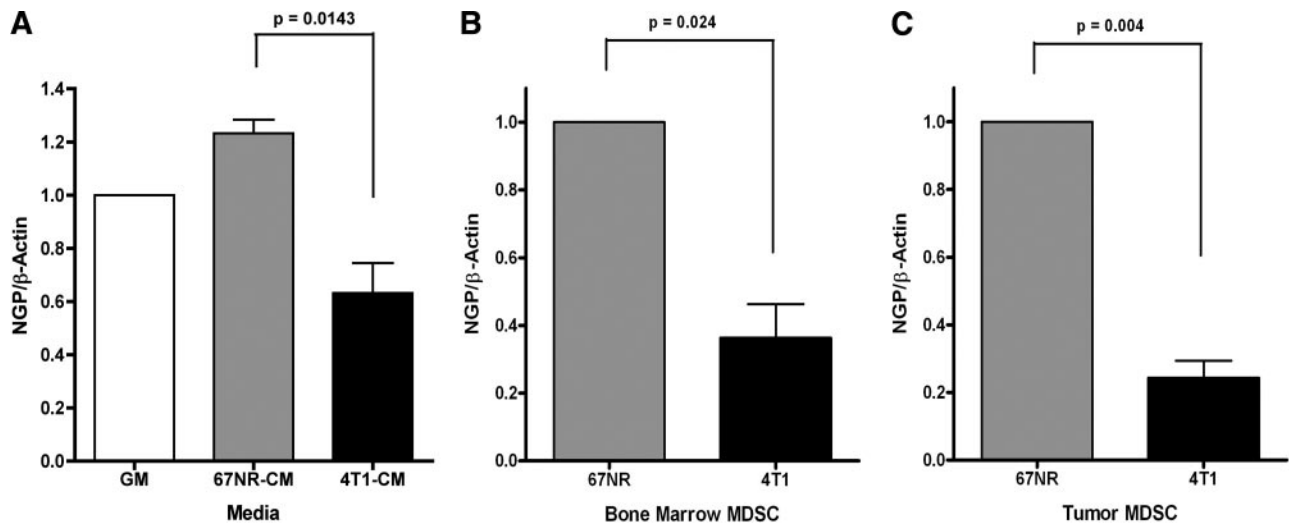
Figure 2. Malignant tumors down-regulate NGP expression in myeloid cells and in MDSCs from bone marrow or tumor tissues. *A*) 32D cells were incubated with conditioned medium collected from 67NR or 4T1 cells or with growth medium (GM) for 24 h. NGP transcript levels were analyzed by real-time PCR. Data represent average $\pm$ sem $\Delta\Delta C_T$ values compared to untreated cells. Each experiment was completed in triplicate and repeated twice. Results are significant by 1-tailed *t* test as indicated by *P* values. *B, C*) Gr1/CD11b cells were isolated from bone marrow (*B*) and tumor tissues (*C*) of mice bearing similar size 67NR tumors or 4T1 tumors by magnetic sorting (*n*=6 mice/group). Data represent average $\pm$ sem $\Delta\Delta C_T$ values compared to MDSCs derived from 67NR tumor-bearing animals. RNA was isolated for real-time PCR to determine NGP expression. Experiments were repeated twice. All data were significant by 2-tailed paired *t* test, $P < 0.05$.

Next, we investigated whether tumor cell-secreted factors could be responsible for NGP suppression associated with malignant tumors. We initially determined the effects of tumor cells on NGP expression in promyelocytes. 32D cells, a myeloid cell line that endogenously expresses NGP, were incubated in conditioned medium from 67NR or 4T1 tumor cells. Real-time PCR

shows that NGP transcript levels were suppressed by ~40%, compared to β-actin, by the presence of medium from 4T1 metastatic tumor cells compared to that derived from the nonmetastatic 67NR cells (**Fig. 2*A***). To confirm the general reduction of NGP in MDSCs associated with malignant 4T1 tumors, we isolated MDSCs from bone marrow and tumor tissues of mice
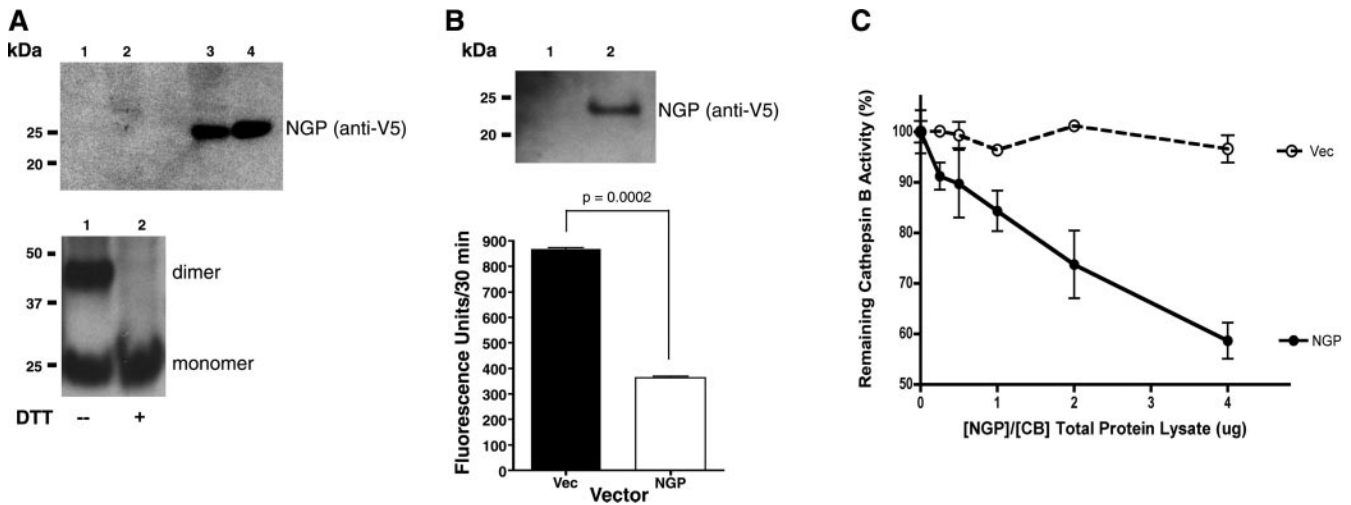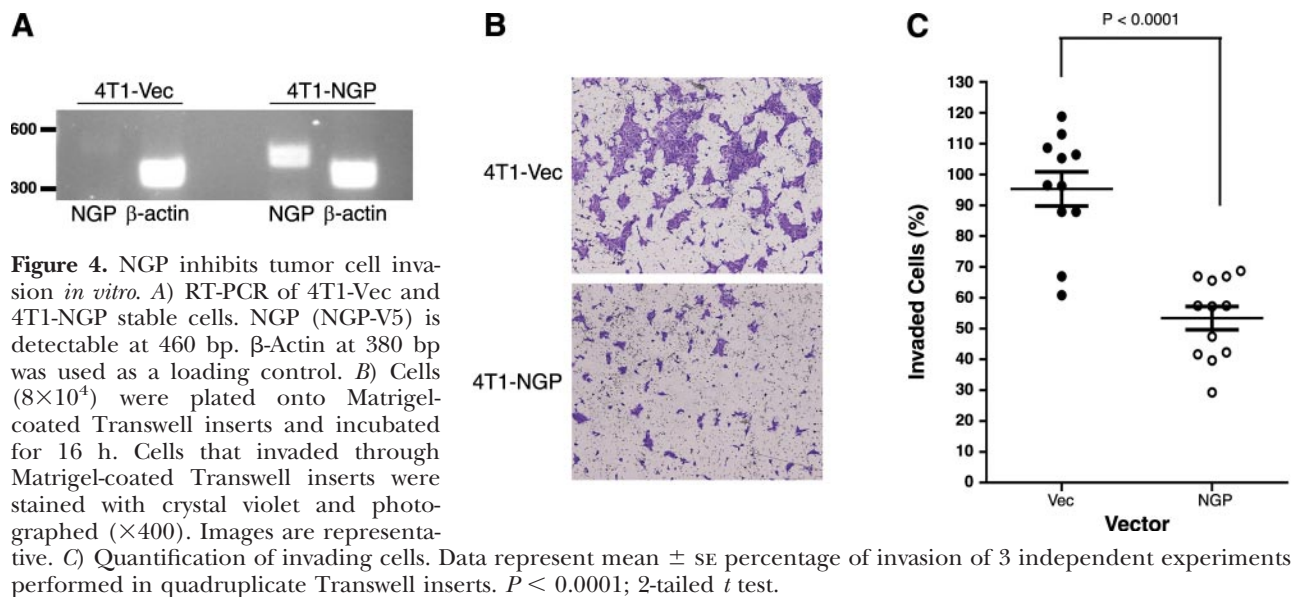

Figure 3. NGP inhibits cathepsin B activity *in vitro*. *A*) NIH-3T3 cells were transfected with empty (lanes 1 and 2) or NGP (lanes 3 and 4) expression vectors for 48 h, respectively. Cell lysate (lanes 1 and 3) and culture medium (lanes 2 and 4) were analyzed for NGP expression by Western blot using V5 antibody (top panel). NGP vector was transfected into HEK 293T for 48 h. Culture medium was analyzed for NGP expression by Western blot without (lane 1) or with (lane 2) 200 μM DTT (bottom panel). *B*) HEK 293T cells were transfected with Vec control (lane 1) or NGP vectors (lane 2) for 48 h. NGP expression was detected in culture medium (top panel). Endogenous cathepsin B activity was measured by fluorogenic substrate RR-AMC. $P = 0.0002$; 2-tailed *t* test (bottom panel). *C*) HEK 293T cells were transfected with either NGP or cathepsin B expression vectors, respectively, for 48 h. Cell lysates were mixed at the ratios indicated. Vec was used as control. Hydrolysis of cathepsin B fluorogenic substrate RR-AMC was measured. Percentage of remaining activity was calculated against the sample without NGP. $P < 0.0001$; 2-way ANOVA. Data are means $\pm$ se of duplicate experiments measured in triplicate.

Figure 4. NGP inhibits tumor cell invasion *in vitro. A*) RT-PCR of 4T1-Vec and 4T1-NGP stable cells. NGP (NGP-V5) is detectable at 460 bp. β-Actin at 380 bp was used as a loading control. *B*) Cells (8×10^4) were plated onto Matrigel-coated Transwell inserts and incubated for 16 h. Cells that invaded through Matrigel-coated Transwell inserts were stained with crystal violet and photographed ($\times$400). Images are representative. *C*) Quantification of invading cells. Data represent mean $\pm$ SE percentage of invasion of 3 independent experiments performed in quadruplicate Transwell inserts. $P < 0.0001$; 2-tailed *t* test.
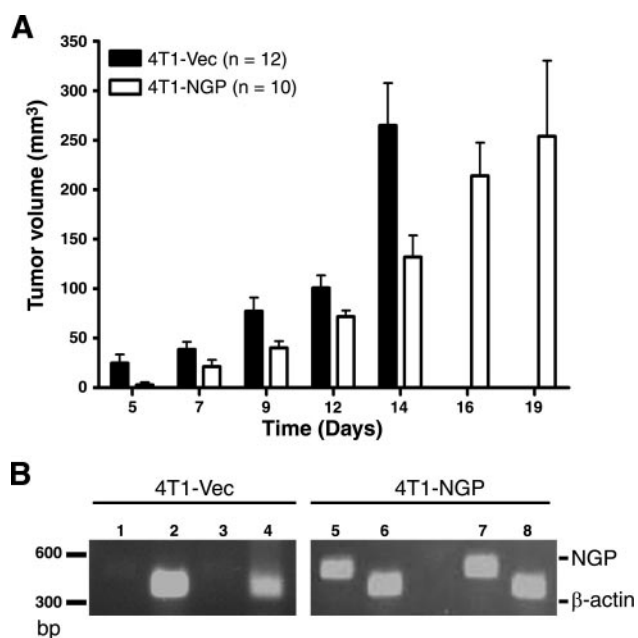
bearing similarly sized 67NR and 4T1 tumors using magnetic cell sorting, followed by real-time PCR analysis of NGP mRNA levels. As expected, we found a similar reduction of NGP in MDSCs isolated from bone marrow and from tumors from animals bearing 4T1 tumors compared to those bearing 67NR tumors. NGP expression in the bone marrow-derived MDSCs decreased by 45% in the 4T1 cohort compared to the relative value of 1 in the 67NR cohort (Fig. 2*B*). The difference in NGP expression 4T1-tumor derived MDSCs was even more pronounced; expression was reduced by 66% compared to 67NR controls (Fig. 2*C*). The data collectively suggest that malignant tumors down-regulate NGP in MDSCs.

NGP is a secreted protein and functions as a cathepsin B inhibitor

We then sequenced full-length NGP using mass spectrometry. Computational analysis of the full-length amino acid sequence using the Conserved Domain Database (16), the Uniprot BLAST Database (17), and Clustal_X alignment suggests that NGP contains a signal peptide, has a putative cystatin domain, and aligns with mouse type II cystatins (Supplemental Fig. S2*A*). The greatest homology is within the N-terminal signal peptide and the cystatin domain encompassing amino acids 40–150 of the NGP sequence (Supplemental Fig. S2*B*). All NGP peptides that were detectable by tandem mass spectrometry are indicated (Supplemental Fig. S3).

To begin exploring the function of NGP, we cloned the full-length gene into a mammalian expression vector with C-terminal V5 and polyhistidine tags. Commonly, type II cystatin proteins contain disulfide bonds, are secreted, and inhibit cysteine proteases, like cathepsin B. We detected NGP in culture medium and cell lysate of 3T3 cells by Western blot with reducing conditions in all lanes, indicating that NGP is indeed

secreted (**Fig. 3*A***, top panel). Similarly, NGP was efficiently expressed in and secreted from HEK 293T cells. Western blot analysis shows secreted NGP as a monomer and a dimer, which migrate to ~25 and ~50 kDa, respectively. The dimer, which is present in nonreducing conditions, was completely abolished with the addition of 200 mM DTT (Fig. 3*A*, bottom panel). These findings show that NGP is secreted as a dimer and

Figure 5. NGP inhibits tumor growth *in vivo. A*) 4T1-NGP or 4T1-Vec cells (5×10^5) were injected into the fourth mammary fat pad of 6–7 wk old female Balb/c mice. Tumor volume was determined based on caliper measurements. Data represent mean $\pm$ SE volume. $P < 0.0001$; 2-way ANOVA. *B*) Confirmation of NGP expression in primary tumors by RT-PCR. Lanes 1–4: 4T1-Vec; lanes 5–8: 4T1-NGP. Lanes 1, 3, 5, 7: NGP; lanes 2, 4, 6, 8: β-actin. NGP (NGP-V5) is indicated at 460 bp and β-actin at 380 bp.
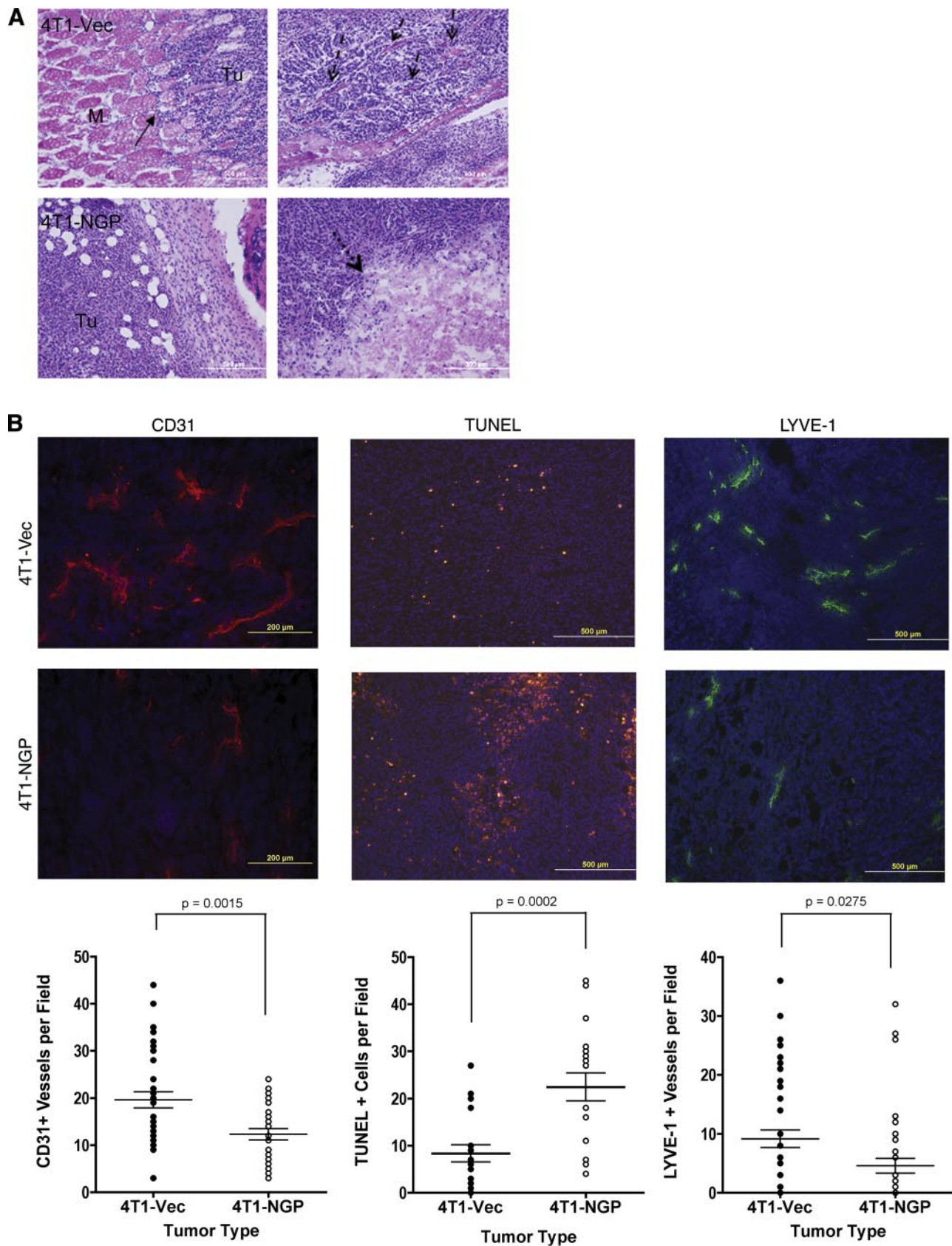
Figure 6. NGP inhibits tumor angiogenesis, lymphangiogenesis, and invasion. *A*) Size-matched tumors were stained with H&E. Solid arrows indicate invasion of tumor cells into adjacent muscle tissue (top left panel). M, muscle; Tu, tumor. Dashed arrows indicate collagen fibers and desmoplasia the 4T1-Vec group (top right panel). Dotted arrows indicate a large necrotic lesion in 4T1-NGP tumor (bottom right panel). Images are representative. M, muscle; Tu, tumor. *B*) Representative images and quanti-

(continued on next page)

monomer, and that the dimer is disulfide linked, as expected for a type II cystatin.

Since NGP contains a putative cystatin-like domain found in endogenous cysteine cathepsin inhibitors, we reasoned that NGP might possess a similar function. We transfected HEK-293T cells with NGP or Vec control. Expression of recombinant NGP was confirmed by Western blotting (Fig. 3B, top panel); cleavage and liberation of cathepsin B fluorogenic substrate, Z-RR-AMC, was reduced to an average of 364 from 868 fluorescence units (Fig. 3B, bottom). Next, we overexpressed cathepsin B and NGP in separate populations of HEK-293 cells, then mixed the two cell lysates. A concentration-dependent inhibition of cathepsin B activity occurred with an increasing ratio of NGP, while total protein lysates containing cathepsin B remained constant. At the greatest ratio of NGP: EV lysates, the remaining cathepsin B activity was ~60% of Vec controls (Fig. 3C). These data collectively demonstrate NGP is a novel cathepsin B inhibitor.

Expression of NGP inhibited tumor cell invasion, but not proliferation *in vitro*

Cathepsin B has been implicated in tumor cell invasion and metastasis in many studies. Aforementioned data identify NGP as an inhibitor of this enzyme, and MDSC NGP expression is negatively correlated to metastasis. Thus, we postulated NGP would adversely affect tumor cell invasion and metastasis. We transfected metastatic 4T1 mammary tumor cells with an NGP expression vector and selected stably expressing clones (4T1-NGP). In the model presented, 4T1 cells are used as a conduit of high-yield NGP production in the tumor microenvironment. After confirmation of NGP expression in 4T1-NGP cells (Fig. 4A), the cells were seeded into culture dishes, and the number of viable cells was determined for 3 consecutive days. Based on the intensity of crystal violet staining for viable cells, the cell density was not changed by the presence of NGP compared to Vec controls or to parental cells (Supplemental Fig. S4A), suggesting that NGP is not likely to have a role in tumor cell proliferation or survival *in vitro*.

Next, we tested 4T1 cell invasion using a Matrigel assay. At 16 h after seeding cells onto growth factor-deprived Matrigel, 4T1-NGP cells showed a striking decrease in the number of invaded cells by microscopy (Fig. 4B). Tumor cell invasion was only ~53% in NGP-expressing cells compared to ~95% in Vec controls (Fig. 4C), which is consistent with the role of cathepsin B in tumor cell invasion and the function of NGP in inhibiting cathepsin B activity.

NGP impairs tumor vascular development and tumor growth, likely through inhibition of cathepsin activity

To further investigate the role of NGP in tumor progression *in vivo*, we implanted 4T1-NGP or 4T1-Vec tumor cells into the mammary fat pad of syngeneic Balb/c mice. NGP significantly inhibited tumor growth compared to Vec controls. The average tumor volume in 4T1-NGP tumors matched that of 4T1-Vec tumors after an additional 5 d. Within 5–14 d, the reduced tumor volume with NGP was decreased (significant by 2-way ANOVA; Fig. 5A). To confirm that NGP expression was not lost due to cellular turnover, tumor tissue lysates were analyzed by RT-PCR. As expected, NGP expression was consistent in 4T1-NGP tumors, but not in Vec controls (Fig. 5B).

Since expression of NGP inhibited tumor growth *in vivo*, we attempted to investigate its mechanism of action. Analysis of tissue sections harvested from size-matched tumors indicates that 4T1-Vec tumors showed greater local invasion into and past the muscle bundle fibers (Fig. 6A, top left image) and showed intercalation of collagen deposits, indicative of desmoplasia (Fig. 6A, top right image). In contrast, no collagen deposition was detectable, but decreased invasion was visible in 4T1-NGP tumors (Fig. 6A, bottom left image), consistent with decreased tumor malignancy. Moreover, tumors expressing NGP had large necrotic lesions at the tumor center (Fig. 6A, bottom right image), in contrast to tumors expressing empty vector, which had no visible necrosis.

Cell death often occurs as a consequence of insufficient nutrient and oxygen delivery to tumors; cathepsins regulate tumor angiogenesis (18). NGP functions as a cathepsin inhibitor; therefore, we examined the effect NGP on tumor angiogenesis. We found that expression of NGP led to a significant reduction in tumor average vascular density from 19.6 to 12.6, as measured by CD31 immunofluorescence (Fig. 6B, left images). Consistently, tumors expressing NGP compared to Vec showed a significant increase in the number of apoptotic cells. The average number of cells per field was 22.4 in 4T1-NGP compared to 8.3 in controls (4T1-Vec), as indicated by TUNEL staining of tumor sections (Fig. 6B, center images). In addition, we measured lymphatic vessel density in tumor sections because lymphatic vessels are important to cell dissemination from primary tumors and subsequent metastasis. We observed a significant reduction of lymphatic vessel density, from 9.1 to 4.6 vessels/field, as measured by LYVE-1 immunofluorescence (Fig. 6B, right images). In contrast, no difference was found in PCNA protein abundance in 4T1 tumor lysates between the two

---

tation of CD31 immunofluorescence, TUNEL fluorescent assay, or LYVE-1 immunofluorescence of size-matched tumors from 5–6 mice/group. Numbers of fields per section analyzed are indicated. Left panels: CD31^{+} vessels were counted in 3 fields/section. $P = 0.0015$; 2-tailed t test. Middle panels: 3 fields/section were counted for TUNEL assay to quantitate apoptotic cells. $P = 0.0002$; 2-tailed t test. Right panels: 5 fields/section were counted for LYVE-1^{+} vessels to quantify lymphatic vessels. $P = 0.0275$; 2-tailed, unpaired t test.

groups, indicating NGP has no significant role in cell proliferation (Supplemental Fig. S4*B*), which is in accordance with observations *in vitro*. These data collectively support that NGP is a negative regulator of tumor vascular development and growth.

To confirm the cathepsin inhibitor activity of NGP *in vivo*, a cysteine cathepsin specific fluorescent probe GB123 (19), which covalently binds to cysteine cathepsins, was intravenously injected into mice with similarly sized tumors prior to imaging. *In vivo* imaging of live animals showed a significant reduction of GB123 probe intensity with NGP expression as an indicator of cysteine cathepsin activity in animals. 4T1-NGP tumors had an average radiance of 29.04 p/s/sr compared to controls, which had 35.98 p/s/sr average radiance (**Fig. 7A**). *Ex vivo* imaging of the excised, intact tumors confirms the reduction, from 1.52 to 0.79 × 10^9 p/s/sr, of the GB123 signal intensity (Fig. 7*B*). In agreement with the *in vivo* and *ex vivo* data, analysis of tumor cell lysates confirmed a significant reduction in cysteine cathepsin activity, in the molecular weight range of cathepsin B, in the presence of NGP expression (Fig. 7*C*). The average fluorescence at the molecular weight corresponding to cathepsin B was only 2.235 in 4T1-NGP tumor lysates, compared to 8.990 in lysates derived from 4T1-Vec tumors. In the same samples, the protein abundance of procathepsin B and cathepsin B is unchanged (Fig. 7*D*). These results suggest that NGP functions as an inhibitor of cathepsin activity, rather than an effector of cathepsin protein expression. NGP expression is correlated negatively to tumor vascular development and tumor growth, likely through inhibition of cathepsin activity.

NGP inhibits tumor cell invasion and pulmonary metastasis *in vivo*

Considering the role of cysteine cathepsins in tumor metastasis and vascular development and taking into account that NGP hinders cathepsin activity, we further investigated the role of NGP in metastasis. After 2–3 wk of primary tumor development in mammary pad, followed by surgical removal of the primary tumors, and 4 wk of recovery and monitoring, pulmonary metastasis was visualized (**Fig. 8A**) and quantitated by counting the number of lung surface metastases and measuring lung weight (Fig. 8*B*, *C*). On average, only 19.7 pulmonary metastases were detectable in the 4T1-NGP group compared to 29.3 in controls, and the lung weight was reduced to 0.15 from 0.19 g in the presence of NGP. In addition, the average size of metastatic tumor foci was reduced to only 0.24 from 0.47 mm in diameter in the Vec control group (Fig. 8*D*, *E*).

Despite careful resection of primary tumors from the mammary pad, regrowth still occurred. Five of 8 mice injected with 4T1-Vec tumor cells showed secondary tumor growth after surgery. In contrast, only 1 of 8 mice in the NGP group had a recurring tumor (**Table 1**). These data are consistent with the negative correlation between NGP expression and tumor cell invasion, which

likely contributes reduced tumor recurrence. Taken collectively, these results support an inhibitory role of NGP in tumor cell invasion and metastasis.

DISCUSSION

MDSCs play a critical role in tumor development. The number of MDSCs is elevated dramatically in cancer patients and tumor-bearing animals and positively correlates with tumor malignancy. On one hand, MDSCs suppress the host immune system to prevent host immune surveillance against tumors; on the other, they infiltrate into tumors, modulate the tumor microenvironment, and promote vascular development, growth, and metastasis (20). Thus, the identification of molecular mediators in MDSCs relevant to tumor malignancy is crucial to further understanding tumor pathology.

The use of mass spectrometry-based proteomics with a mouse model of metastatic potential led us to identify a novel MDSC-derived protein, NGP. We found that NGP possesses antitumor and antimetastasis functions. Our data indicate that malignant tumor conditions suppress NGP expression in MDSCs. In turn, stable expression of NGP in tumor cells leads to decreased cathepsin activity and suppressed tumor progression and metastasis through modulation of angiogenesis, lymphanogenesis, and cell death.

NGP was identified initially as an azure positive granule protein in myeloid bone marrow stem cells. MDSCs are derived from bone marrow myeloid; thus, the presence of NGP in MDSCs was somewhat anticipated. However, a reduction of NGP in MDSCs in the presence of metastatic tumors was quite remarkable. Reduction of NGP expression in MDSCs might illustrate a new mechanism utilized by the host response to metastatic tumors, which, unfortunately, benefits tumor progression. Our findings that malignant tumor conditioned medium suppresses NGP expression in myeloid cells indicates that a secreted factor from tumors might be responsible for down-regulation of this gene.

Peptide sequence analysis by tandem mass spectrometry suggests NGP belongs to the type II cystatin family, members of which function as cathepsin inhibitors. Genetic ablation of cathepsins reduces tumor burden in multiple tumor models, and also a negative correlation exists between cystatins and tumor burden in patients with cancer (21, 22). Tumor progression is regulated not only by increased protease activity but also down-regulation of protease inhibitors (23). Therefore, the reduction of NGP in the presence of the metastatic tumor model in the present study might be in accordance with observations made for other cystatins.

Although NGP is an MDSC-derived protein and is secreted, we wanted to determine whether it had a direct effect on facets of tumor development similar to studies conducted with cystatin M/E or cystatin C. Cystatins that are intracellularly expressed or endocytosed by malignant tumor cells inhibit cysteine cathep-
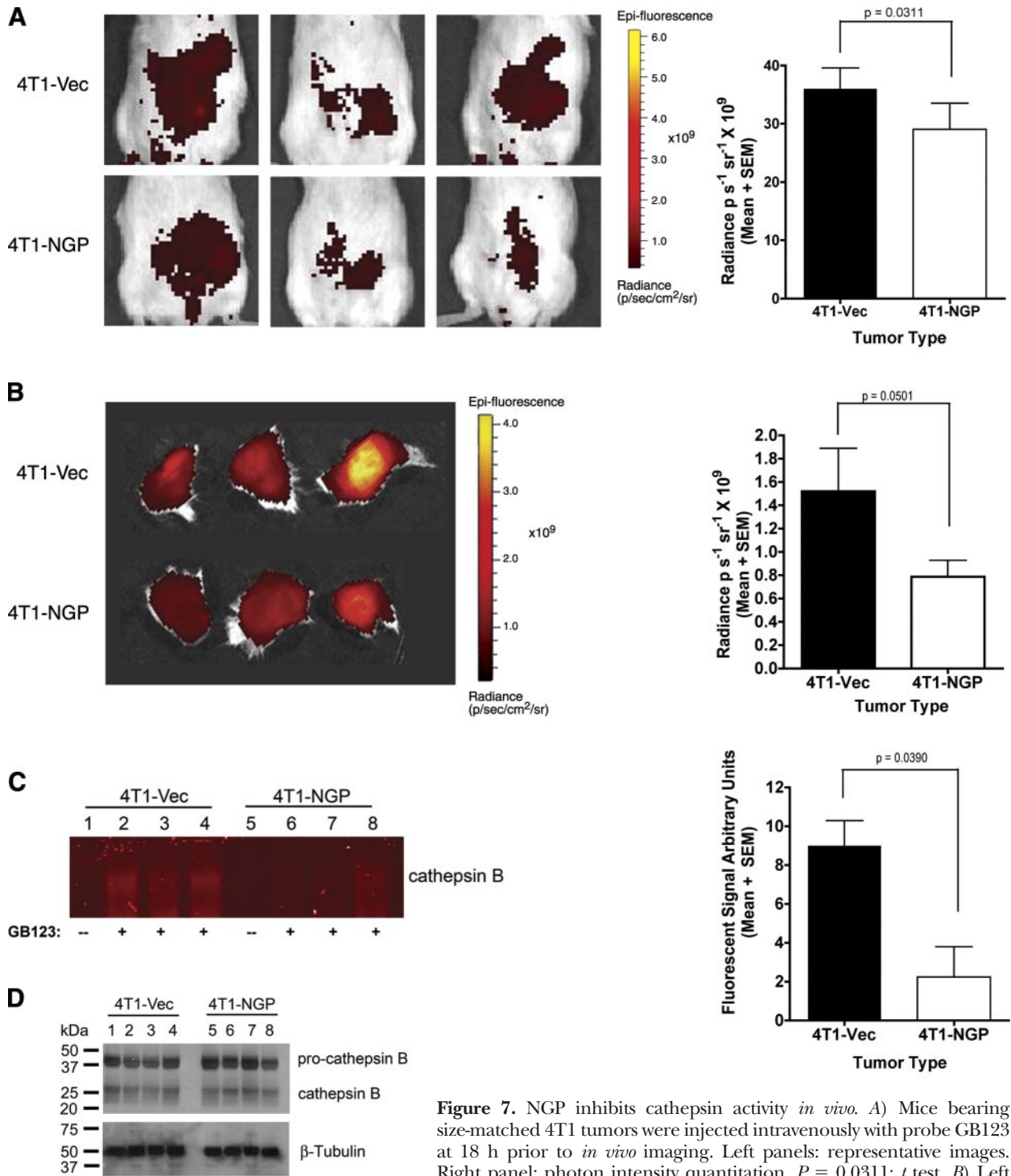
Figure 7. NGP inhibits cathepsin activity *in vivo. A*) Mice bearing size-matched 4T1 tumors were injected intravenously with probe GB123 at 18 h prior to *in vivo* imaging. Left panels: representative images. Right panel: photon intensity quantitation. $P = 0.0311$; *t* test. *B*) Left panel: whole tumors were removed surgically and imaged for cathepsin activity by GB123 probe intensity. Right panel: quantification of data. $P = 0.05$; *t* test. *C*) Left panel: equal amounts of total protein from tumor lysates were separated by PAGE; probe fluorescence at cathepsin B molecular weight was visualized on a flatbed scanner. Lane 1–4: 4T1-Vec, lane 1 without probe and lanes 2–4 with probe; lanes 5–8: 4T1-NGP, lane 5 without probe and lanes 6–8 with probe. Right panel: intensities of the labeled bands were quantified and plotted as means ± SE. $P = 0.039$; *t* test. *D*) Protein samples identical to those in *C* were analyzed by Western blot for cathepsin B protein. β-Tubulin was used as a loading control. Each analysis utilized size-matched tumors from 3 mice/group.

sins (24). We sought to directly determine NGP's effects while restricting its expression to the tumor microenvironment. In our model, ectopic expression of NGP in tumor cells acts as a constant source of protein production within the tumor microenviron-

ment. We found that expression of NGP led to a significant suppression of tumor growth; but, unlike many endogenous inhibitors that control tumor cell proliferation, NGP had no such effect. Instead, NGP expression leads to increased apoptosis and necrosis in
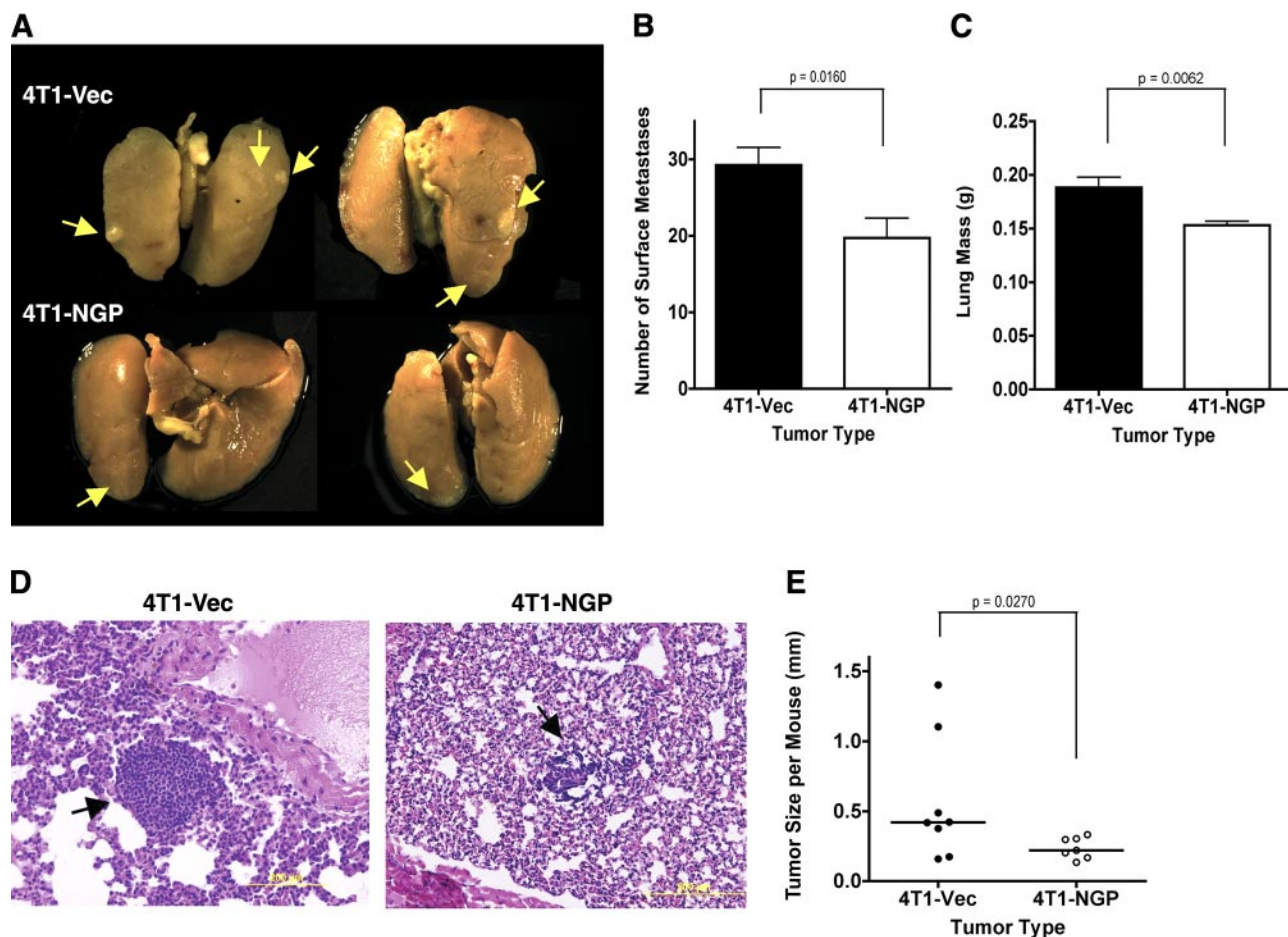
Figure 8. NGP expression inhibits pulmonary metastasis of mammary tumors. *A*) Representative images of lung metastases after fixation in Bouin's fixative. Arrows indicate visible lung surface metastases. *B*) Number of visible surface metastases of lung tissues. $P = 0.0160$; 2-tailed *t* test. *C*) Measured weight of freshly harvested lungs. $P = 0.0062$; 2-tailed *t* test. *D*) Representative images of H&E-stained sections of lung tissues. *E*) Quantification of metastatic tumor diameter from H&E-stained sections. $P = 0.0242$; 2-tailed Welch's *t* test.

addition to delayed tumor growth. Simultaneous loss of cathepsins B and L leads to prolific apoptosis in knockout mice (25). Therefore, NGP-mediated cell death could be a direct effect of cathepsin B inhibition.

Elevated cell death could also result from insufficient delivery of nutrients and oxygen due to an inhibition of tumor angiogenesis, as observed in the present study. NGP inhibition of cathepsin B might be a leading cause for decreased neovascularization. In fact, cysteine and serine cathepsin activity are increased within the angiogenic vasculature, and vascular formation is driven partly

by cathepsin activity through regulation of VEGF bioavailability within the extracellular matrix. Vessel density is reduced in cathepsin B-deficient mice and in the presence of cathepsin inhibitors (18, 26). The vascular basement membrane is composed of extracellular matrix proteins, cleaved by active cathepsin B, facilitating robust angiogenesis (27). Thus, NGP could impair angiogenesis through blocking cysteine cathepsin activities.

Reduction of lymphangiogenesis in NGP-expressing tumor cells could also contribute to impaired tumor metastasis. NGP inhibition of cathepsin B might also be

TABLE 1. *Incidence of tumor recurrence*

	4T1-Vec			4T1-NGP		
Type	Tumor	No tumor	Incidence (%)	Tumor	No tumor	Incidence (%)
Primary	8	0	100	8	0	100
Recurrent	5	3	63	1	7	13

After primary tumor excision, animals were monitored closely for tumor recurrence in the fourth mammary fat-pad. Regrowth of palpable tumors in the mammary pad was determined 4 wk after removal of the primary tumor. Difference in recurrence is significant by 2-tailed χ^2, $P = 0.0389$.

a leading cause for decreased lymphatic vessel development, since cathepsins B and L are associated with lymphatic vessel density (28). Cathepsin B is one of the key proteases involved in tumor progression. Overlapping inhibitor and substrate specificities are known for the cysteine proteases and the specificity of NGP is currently being determined.

Cathepsins are active intra-, extra-, and pericellularly (29). Type II cystatins are often secreted as an inactive form and activated on reduction *in vitro* (30). We show that NGP is in fact secreted as a monomer and a disulfide-linked homodimer and that it contains a putative cystatin domain. NGP can also inhibit cathepsin B activity within malignant tumors, as indicated by reduction of GB123 fluorescence in intact tumors and lysates. Down-regulation of NGP might allow MDSCs to exhibit a greater "protumor" phenotype. NGP might exist in different forms, reflecting different stages in protein maturation as it is expressed and post-translationally modified, held in organelles, then finally secreted and reduced to an active form. The reduced, secreted form might in fact be responsible for the inhibition of cysteine cathepsins that affect angiogenesis and metastasis, which warrants further investigation. To our knowledge, this study is the first to indicate that MDSCs can produce cysteine cathepsin inhibitors; further exploration of this model will aid in determining the protumor role of MDSCs.

In summary, this study reveals expression of NGP in MDSCs and identifies a novel function of this cystatin-like secreted protein in tumor development and metastasis. Note that the majority of studies focus on tumor cell-derived cystatins. Our findings demonstrate that host-derived MDSCs are also an important source of such factors. Presence of malignant tumor cells suppresses NGP expression in MDSCs; overexpression of NGP is correlated to reduced cathepsin B activity in tumor cells. NGP negatively regulates tumor growth, invasion. and metastasis; it suppresses tumor angiogenesis and lymphangiogenesis but increases apoptosis and necrosis. The discreet roles of NGP in these processes indicate new avenues by which MDSCs mediate tumor progression and metastasis. FJ

REFERENCES

1. Gabrilovich, D. I., and Nagaraj, S. (2009) Myeloid-derived suppressor cells as regulators of the immune system. *Nat. Rev. Immunol.* **9,** 162–174
2. Almand, B., Clark, J. I., Nikitina, E., van Beynen, J., English, N. R., Knight, S. C., Carbone, D. P., and Gabrilovich, D. I. (2001) Increased production of immature myeloid cells in cancer patients: a mechanism of immunosuppression in cancer *J. Immunol.* **166,** 678–689
3. Yang, L., DeBusk, L. M., Fukuda, K., Fingleton, B., Green-Jarvis, B., Shyr, Y., Matrisian, L. M., Carbone, D. P., and Lin, P. C. (2004) Expansion of myeloid immune suppressor Gr+CD11b+ cells in tumor-bearing host directly promotes tumor angiogenesis. *Cancer Cell* **6,** 409–421
4. Diaz-Montero, C. M., Salem, M. L., Nishimura, M. I., Garrett-Mayer, E., Cole, D. J., and Montero, A. J. (2009) Increased circulating myeloid-derived suppressor cells correlate with clinical cancer stage, metastatic tumor burden, and doxorubicin-cyclophosphamide chemotherapy. *Cancer Immunol. Immunother.* **58,** 49–59
5. Shojaei, F., Wu, X., Malik, A. K., Zhong, C., Baldwin, M. E., Schanz, S., Fuh, G., Gerber, H.-P., and Ferrara, N. (2007) Tumor refractoriness to anti-VEGF treatment is mediated by CD11b+Gr1+ myeloid cells. *Nat. Biotechnol.* **25,** 911–920
6. Sinha, A. A., Quast, B. J., Wilson, M. J., Fernandes, E. T., Reddy, P. K., Ewing, S. L., and Gleason, D. F. (2002) Prediction of pelvic lymph node metastasis by the ratio of cathepsin B to stefin A in patients with prostate carcinoma. *Cancer* **94,** 3141–3149
7. Barrett, A. J. (1986) The cystatins: a diverse superfamily of cysteine peptidase inhibitors. *Biomed. Biochim. Acta* **45,** 1363–1374
8. Kioulafa, M., Balkouranidou, I., Sotiropoulou, G., Kaklamanis, L., Mavroudis, D., Georgoulias, V., and Lianidou, E. S. (2009) Methylation of cystatin M promoter is associated with unfavorable prognosis in operable breast cancer *Int. J. Cancer* **125,** 2887–2892
9. Parker, B. S., Ciocca, D. R., Bidwell, B. N., Gago, F. E., Fanelli, M. A., George, J., Slavin, J. L., Moller, A., Steel, R., Pouliot, N., Eckhardt, B. L., Henderson, M. A., and Anderson, R. L. (2008) Primary tumour expression of the cysteine cathepsin inhibitor Stefin A inhibits distant metastasis in breast cancer *J. Pathol.* **214,** 337–346
10. Sevenich, L., Schurigt, U., Sachse, K., Gajda, M., Werner, F., Müller, S., Vasiljeva, O., Schwinde, A., Klemm, N., Deussing, J., Peters, C., and Reinheckel, T. (2010) Synergistic antitumor effects of combined cathepsin B and cathepsin Z deficiencies on breast cancer progression and metastasis in mice. *Proc. Natl. Acad. Sci. U. S. A.* **107,** 2497–2502
11. Vasiljeva, O., Papazoglou, A., Krüger, A., Brodoefel, H., Korovin, M., Deussing, J., Augustin, N., Nielsen, B. S., Almholt, K., Bogyo, M., Peters, C., and Reinheckel, T. (2006) Tumor cell-derived and macrophage-derived cathepsin B promotes progression and lung metastasis of mammary cancer. *Cancer Res.* **66,** 5242–5250
12. Moscinski, L. C., and Hill, B. (1995) Molecular cloning of a novel myeloid granule protein. *J. Cell. Biochem.* **59,** 431–442
13. Gombart, A. F., Kwok, S. H., Anderson, K. L., Yamaguchi, Y., Torbett, B. E., and Koeffler, H. P. (2003) Regulation of neutrophil and eosinophil secondary granule gene expression by transcription factors C/EBP epsilon and PU. 1. *Blood* **101,** 3265–3273
14. Friedman, D. B., and Lilley, K. S. (2008) Optimizing the difference gel electrophoresis (DIGE) technology. *Methods Mol. Biol.* **428,** 93–124
15. Aslakson, C. J., and Miller, F. R. (1992) Selective events in the metastatic process defined by analysis of the sequential dissemination of subpopulations of a mouse mammary tumor. *Cancer Res.* **52,** 1399–1405
16. Marchler-Bauer, A., Anderson, J. B., Cherukuri, P. F., DeWeese-Scott, C., Geer, L. Y., Gwadz, M., He, S., Hurwitz, D. I., Jackson, J. D., Ke, Z., Lanczycki, C. J., Liebert, C. A., Liu, C., Lu, F., Marchler, G. H., Mullokandov, M., Shoemaker, B. A., Simonyan, V., Song, J. S., Thiessen, P. A., Yamashita, R. A., Yin, J. J., Zhang, D., and Bryant, S. H. (2005) CDD: a Conserved Domain Database for protein classification. *Nucleic Acids Res.* **33,** D192–196
17. Wu, C. H., Apweiler, R., Bairoch, A., Natale, D. A., Barker, W. C., Boeckmann, B., Ferro, S., Gasteiger, E., Huang, H., Lopez, R., Magrane, M., Martin, M. J., Mazumder, R., O'Donovan, C., Redaschi, N., and Suzek, B. (2006) The Universal Protein Resource (UniProt): an expanding universe of protein information. *Nucleic Acids Res.* **34,** D187–191

18. Chang, S. H., Kanasaki, K., Gocheva, V., Blum, G., Harper, J., Moses, M. A., Shih, S. C., Nagy, J. A., Joyce, J., Bogyo, M., Kalluri, R., and Dvorak, H. F. (2009) VEGF-A induces angiogenesis by perturbing the cathepsin-cysteine protease inhibitor balance in venules, causing basement membrane degradation and mother vessel formation. *Cancer Res.* **69,** 4537–4544

19. Blum, G., von Degenfeld, G., Merchant, M. J., Blau, H. M., and Bogyo, M. (2007) Noninvasive optical imaging of cysteine protease activity using fluorescently quenched activity-based probes. *Nat. Chem. Biol.* **3,** 668–677

20. Yang, L., Huang, J., Ren, X., Gorska, A. E., Chytil, A., Aakre, M., Carbone, D. P., Matrisian, L. M., Richmond, A., Lin, P. C., and Moses, H. L. (2008) Abrogation of TGF beta signaling in mammary carcinomas recruits Gr-1+CD11b+ myeloid cells that promote metastasis. *Cancer Cell* **13,** 23–35

21. Chen, X., Cao, X., Dong, W., Xia, M., Luo, S., Fan, Q., and Xie, J. (2010) Cystatin M expression is reduced in gastric carcinoma and is associated with promoter hypermethylation. *Biochem. Biophys. Res. Commun.* **391,** 1070–1074

22. Wegiel, B., Jiborn, T., Abrahamson, M., Helczynski, L., Otterbein, L., Persson, J. L., and Bjartell, A. (2009) Cystatin C is downregulated in prostate cancer and modulates invasion of prostate cancer cells via MAPK/Erk and androgen receptor pathways. *PLoS ONE* **4,** e7953

23. Cox, J. L. (2009) Cystatins and cancer. *Front. Biosci.* **14,** 463–474

24. Ekstrom, U., Wallin, H., Lorenzo, J., Holmqvist, B., Abrahamson, M., and Aviles, F. X. (2008) Internalization of cystatin C in human cell lines. *FEBS J.* **275,** 4571–4582

25. Felbor, U., Kessler, B., Mothes, W., Goebel, H. H., Ploegh, H. L., Bronson, R. T., and Olsen, B. R. (2002) Neuronal loss and brain atrophy in mice lacking cathepsins B and L. *Proc. Natl. Acad. Sci. U. S. A.* **99,** 7883–7888

26. Hu, L., Roth, J. M., Brooks, P., Luty, J., and Karpatkin, S. (2008) Thrombin up-regulates cathepsin D which enhances angiogenesis, growth, and metastasis. *Cancer Res.* **68,** 4666–4673

27. Cavallo-Medved, D., Rudy, D., Blum, G., Bogyo, M., Caglic, D., and Sloane, B. F. (2009) Live-cell imaging demonstrates extracellular matrix degradation in association with active cathepsin B in caveolae of endothelial cells during tube formation. *Exp. Cell. Res.* **315,** 1234–1246

28. Niedergethmann, M., Wostbrock, B., Sturm, J. W., Willeke, F., Post, S., and Hildenbrand, R. (2004) Prognostic impact of cysteine proteases cathepsin B and cathepsin L in pancreatic adenocarcinoma. *Pancreas* **29,** 204–211

29. Sloane, B. F., Rozhin, J., Johnson, K., Taylor, H., Crissman, J. D., and Honn, K. V. (1986) Cathepsin B: association with plasma membrane in metastatic tumors. *Proc. Natl. Acad. Sci. U. S. A.* **83,** 2483–2487

30. Colbert, J. D., Plechanovová, A., and Watts, C. (2009) Glycosylation directs targeting and activation of cystatin f from intracellular and extracellular sources. *Traffic* **10,** 425–437